Towards a multi-scale virtual heart model

Zexian Wang, François Varray, Patrick Clarysse, Isabelle E. Magnin

Towards a multi-scale virtual heart model

Zexian Wang*, François Varray*, Patrick Clarysse* and Isabelle E. Magnin*
*CREATIS UMR 5220, U1206
Univ Lyon, INSA-Lyon,Université Claude Bernard Lyon 1, UJM-Saint Etienne
Lyon, France
zexian.wang@creatis.insa-lyon.fr

***Abstract*—This paper presents a three-dimensional multiscale structure and object-oriented model to generate a synthetic heart. This model consists of a series of elementary objects at different resolution level from the macro- to the micro-scale. Each object is described by a vector of attributes. The shapes and size of the components of the tissue are inspired from Synchrotron Radiation Phase micro-Computed Tomography (SR-PCT) of human left ventricle wall samples. To enhance the similarity between the model and the experimental data, we use a Free-Form Deformation (FFD) technique to deform each object. Our first results demonstrate that the model can simulate realistic voxel-based elementary objects and simulate experimental data and shapes. The hierarchical graph structure of the model that includes inter level relationships has a strong potential interest.**

***Index Terms*—multiscale modeling, cardiac tissue, geometric model, deformable model, graph, feature vectors**

I. Introduction

Cardiovascular diseases remain the main cause of death in developed countries, which deprive yearly the lives of over 17 millions people all over the world (WHO). Advanced imaging techniques have enhanced the clinical diagnosis accuracy of cardiovascular diseases. A better knowledge of the 3D arrangement of the structures present in the heart could help overcoming some of the remaining limitations. A way to reach that goal, consists in developing 3D models of the heart to contribute to the understanding of the relationships between the mechanical and hemodynamical functions as well as the structural changes due to normal and pathological cardiac remodeling. The heart is a complex, mobile and deformable functional system and due to its complexity, most models focus mainly on one aspect of it.

In the past years, 3D geometric and deformable models [1], [2] have been proposed. Models also allowing the analysis of cardiac movement [3], simulation of water diffusion [4] and even computer clinical diagnosis [5].

Multiscale modeling fits biological tissue due to the inherent hierarchical structure of its elementary objects and their coupling from one scale to the next. Recently, various multiscale models [6] have been proposed to study the structural relationships in a heart [7], [8], the cardiac electrophysiology [9]–[12], its hemodynamics [13] or mechanical function [14], [15]. However, the cardiac structure is complex. It is composed of a series of embedded multiscale elementary objects working together. Data integration across spatial and functional scales is the subject of significant research efforts, since the simulation of a functional heart is one of the most intractable problems. Most studies are often limited by the anisotropy and/or low resolution of data as in Diffusion Tensor Imaging (DTI) [16] or Polarized Light Imaging (PLI) [17]. The recent work of our group [18]–[21] imaging human cardiac tissue with phase contrast SR-PCT, provides some quantitative knowledge about the 3D arrangement of the cellular and extra-cellular matrix at a micrometric isotropic spatial resolution.

In this paper, we propose a three-dimensional multiscale model made of a series of elementary objects of the heart, crossing the scales from the global level (macro-scale) to the tissue level (micro-scale). The paper is organized as follows. First, we give the overall description of our multiscale model with its hierarchical graph structure and the relationships between its elementary objects described by geometric voxel-based elementary models. Second, we introduce the transform used to control the deformation process of the geometric models at each scale. In the results part, we demonstrate some initial results at the tissue scale involving virtual cells, bundles (cellular matrix) and cleavage planes (extracellular matrix). A discussion and a conclusion end the paper.

II. Multiscale Model

The proposed model contains the main anatomical elementary objects of the heart at five levels from the macro- to the micro-scale. It includes the ventricles, atria, sheets, bundles and myocytes as well as the extracellular matrix such as the cleavage planes, endocardium, epicardium and perimysium. The relations between the objects and the levels are presented in Fig. 1. We consider each element of the heart as an object, like a node in a net. These objects can be simply connected or completely nested within each other. In the vertical direction of the structure, an object belonging to level N contains the object of level $N+1$. Meanwhile, the spatial resolution varies from centimeter to micrometer. In the horizontal direction, all objects belonging to the same level are mutually connected. This description generates a 3D hierarchical net structure. In Fig. 1, the blue arrows demonstrate the affiliation while the green ones indicate connectivity.

A. A hierarchical nested structure

Level 1 is the root (macro-scale) of the model. It includes anatomical features as the epicardium, endocardium and myocardium of each atrium and ventricle and the septum. The global epicardial surface consists in four connected epicardial sub-regions (objects). This level addresses functional issues

such as global shape deformation or cavities volume changes along the cardiac cycle.

Level 2 is focused on the cardiac tissue. It concerns the extracellular matrix (ECM) with the sheets and cleavage planes in relation with the laminar structure and the mechanical properties of the tissue.

Level 3 mainly deals with the cellular matrix (CM) with its bundles of myocytes embedded in the ECM. The local twist and sliding of the ECM and CM arising at levels 2 and 3 contribute to the global deformation of the myocardium.

Level 4 is the cellular level at the scale of individual myocytes.

Level 5 (micro-scale) corresponds to the leafs of the graph model described by voxels.

B. An object-oriented description

Each level N contains a series of objects described by a feature vector V of parameters (Fig. 2). This vector contains intrinsic, physical and extrinsic parameters, inspired from anatomical knowledge and statistical measurements. Among those features, we find the location, affiliation, shape, connectivity and physical parameters as electrical or acoustical impedance, involved in diverse imaging techniques. A vector V of attributes is defined as $V(x, y, z; l, r, \theta, \phi; adj...; ...)$ where (x, y, z) stands for the coordinates of the center of the myocyte, l its length and r its radius if the geometric model of the myocyte is a cylinder. The angles θ, ϕ define the 3D orientation of the main axis of the cylinder (myocyte) and adj describes the properties of adjacency with neighbouring structures. Fig. 3 illustrates an example of the software structure associated to the elementary object "myocyte". Besides the attributes, functions can be called to achieve different purposes. Each object at level N inherits the attributes from its parents of level $N-1$.

C. Voxel-Based Models

We use the voxel as basic unit. Indeed, voxel-based models are well adapted to represent the complex structures of the human anatomy. Moreover, they are flexible and able to scale in size and deform to match any required dimension or deformation [22]. To set up voxel-based models, we first need to identify the boundaries between the objects contained in the model. Second, we need to label all voxels belonging to the same organ with a unique identification. Thus, each voxel is identified and distinguished from the others. Voxels belonging to the same object are part of the same class.

III. Deformable Geometric Model

The heart is a functional elastic organ, which undergoes large overall deformations of the shape and subtle internal 3D rearrangements of the tissue along the successive cardiac cycles. Thus, geometric models for each elementary object must account for deformation. This explains why, after setting the basic geometric models, we immediately introduce their deformable properties. Among various possible approaches, we select the Free-Form Deformation (FFD) technique because

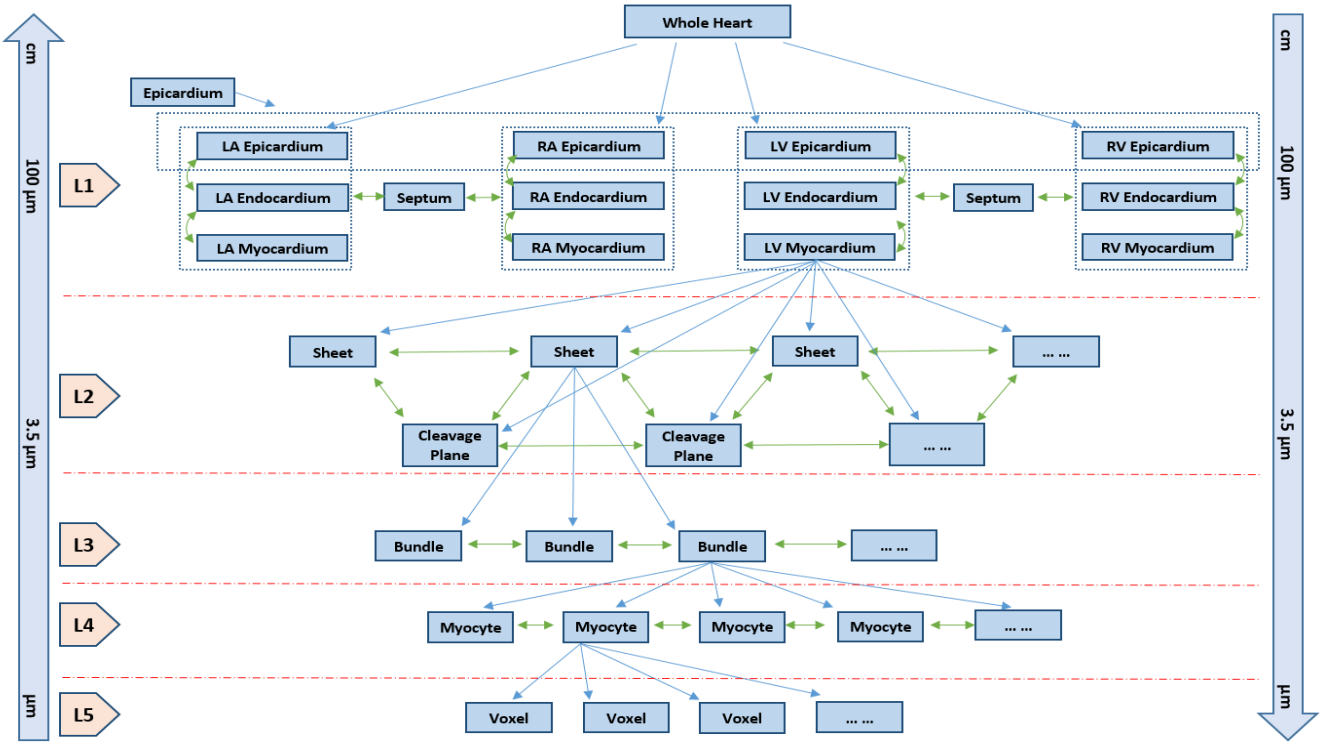

Fig. 1. Structure of the multiscale model. LA: Left Atrium. RA: Right Atrium. LV: Left Ventricle. RV: Right Ventricle. L1-L5: Levels corresponding to the scales of the model.

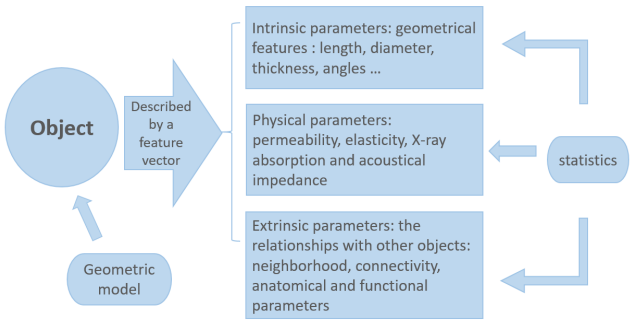

Fig. 2. Structure of each elementary object.

```
Myocyte
Attributes:
   index
   pos   % struct('x','y','z')
   attr   % struct('lvl1','lvl2', 'lvl3')
   geopara   % struct('len','dia','theta','phi')
   adjpara   % struct('adj_idx1','adj_idx2',...)
   imgpara
   modpara
Methods:
   myocyte()
   show()
   ...
```

Fig. 3. Elementary object-myocyte with its attributes.

of its many advantages. We introduce FFD at each level of the model. In this section, we brief recall the principle of FFD.

A. Free-Form Deformation

The Free-Form Deformation is a deformation technique proposed by Thomas W. Sederberg to deform solid geometric models [23]. The FFD re-defines the location of a geometric object in a local coordinate system and uses a set of control points and a set of Bernstein polynomials to build a relationship between the objects and the control points. This relationship is represented by a tri-variate tensor product of polynomials which is an important notion in approximation theory and guarantees the smoothness in the deformation. When the locations of the control points are moved, the shape of the object is changed as well. The free-form movements of the controls points result in the deformation of the shape.

The FFD technique is a useful and frequently used deformation method because of its several important properties. FFD does not require any specific type or shape for the objects. It is possible to control the volume of the objects during the FFD process. The parametric objects remain parametric after FFD. It is possible to apply several FFDs on an object in a piece-wise manner with the cross-boundary derivative continuity being maintained.

Based on the above statements, we use the FFD technique to transform the shapes of each elementary object making the heart from the macro- to the micro-scale. A local coordinate system $(S,T,U) \in \mathbb{R}^3$ is defined at the origin of the rectangular box containing the data. The dimension of the domain is defined by the coordinate range (min-max) in the 3 directions. In this local coordinate system, the original location of data X within the domain can be expressed as:

$$X = X_0 + s\vec{S} + t\vec{T} + u\vec{U} \tag{1}$$

where X_0 states for the origin of the rectangular box and the coordinates (s,t,u) of any point inside the data can be calculated by:

$$(s,t,u) = \left(\frac{\vec{T}\times\vec{U}\,(X-X_0)}{\vec{T}\times\vec{U}\cdot\vec{S}}, \frac{\vec{S}\times\vec{U}\,(X-X_0)}{\vec{S}\times\vec{U}\cdot\vec{T}}, \frac{\vec{S}\times\vec{T}\,(X-X_0)}{\vec{S}\times\vec{T}\cdot\vec{U}} \right) \tag{2}$$

with $s \in [0,1]$, $t \in [0,1]$, $u \in [0,1]$, where "$\times$" and "$\cdot$" denote the outer and inner products of vectors.

The second step consists in immersing the data into a 3D grid of control points P of size $(l+1)\times(m+1)\times(n+1)$. Then, the coordinates of each control point P_{ijk} is given by:

$$P_{ijk} = X_0 + \frac{i}{l}\vec{S} + \frac{j}{m}\vec{T} + \frac{k}{n}\vec{U} \tag{3}$$

where i, j, k being the index of the control point in the S, T and U directions, respectively.

The displacement of the control points deforms the object, while the trivariate tensor product Bernstein polynomial defines the deformation function:

$$X_{ffd} = \sum_{i=0}^{l}\sum_{j=0}^{m}\sum_{k=0}^{n} C_l^i (l-s)^{l-i} s^i C_m^j (l-t)^{m-j} t^j C_n^k (l-u)^{n-k} u^k P_{ijk} \tag{4}$$

with P_{ijk} the moved control points and C_l^i, C_m^j, C_n^k the 1D Bernstein polynomial.

B. High-Resolution Geometric Model

We consider the cell (myocyte) as an elementary object of our cardiac tissue model, represented by a cylinder. From histological studies [24] and SR-PCT [18], [20], [21] we know that the myocytes are organised in "bundles" containing a limited number of myocytes. We define the "bundle" as a geometric object containing a limited series of myocytes. The shape of a bundle of myocytes, in a biological tissue, could be compared to a "rugby" ball with a thinner section at its extremities. To build such a realistic bundle, we start from a cylindrical bundle model (initial object) containing a limited series of parallel myocytes (cylinders) and we define a morphing transform to go from this initial shape to the final ellipsoidal shape.

We use a cylinder of radius R_b and length L_b to simulate a bundle (5).

$$\frac{x^2}{R_b^2}+\frac{y^2}{R_b^2}<1, |z|<\frac{L_b}{2}, R_b>0, L_b>0 \tag{5}$$

At first, the objective form is supposed to be a truncated ellipsoid cylinder, whose original equation is:

$$\frac{x^2}{(R_x)^2}+\frac{y^2}{(R_y)^2}+\frac{z^2}{(R_z)^2}<1, R_x>0, R_y>0, R_Z>0 \tag{6}$$

with the circular section of the cylinder lying in the (x, y) plane and the height in the z direction. The cylinder is centered in $(0, 0, 0)$. The 3D transform to go from a cylinder to an ellipsoid is not straightforward, so we decide to deform the initial cylinder layer by layer along the z direction. This strategy allows us to precisely handle and control the parameters of the output truncated ellipsoid. We now define the deformation of a circle of radius R_b towards an ellipse of equation:

$$\frac{x^2}{R_x^2}+\frac{y^2}{R_y^2}=1-\frac{z^2}{R_z^2}<1 \tag{7}$$

We can rewrite this equation as:

$$\frac{x^2}{(R_x c)^2}+\frac{y^2}{(R_y c)^2}=1 \tag{8}$$

where $c=\sqrt{1-k^2/R_z^2}$ is the weighting coefficient of the radius along the x and y directions. It means that the radius of the k-th layer is c times the radius of the 0-th layer. Thus, we can calculate the weighting parameters t_x and t_y of the deformation used to modify the original radius of the circle as well as the coordinates of the control points along the x and y direction:

$$t_x=\frac{R_x c}{R_b}, t_y=\frac{R_y c}{R_b} \tag{9}$$

In a realistic tissue, the bundle's shape is more like a twisted noisy truncated ellipsoid. We adapt the model to create such an effect. We keep a layer-by-layer process. We define a rotation and add a Gaussian noise to the control points controlling each layer. The rotation degree A_z in function of z is defined as:

$$A_z=A_{rotation}\times z \tag{10}$$

where $A_{rotation}$ is an arbitrary angle. We define a Gaussian model of noise of mean (μ_x, μ_y) and standard deviation (σ_x, σ_y) to perturb the location of each control point belonging to the layer $(x, y)_{cp}$. The noisy locations of the control point $(x, y)_{cpn}$ are given by:

$$(x,y)_{cpn}=(x,y)_{cp}+\left(\frac{1}{\sigma_x\sqrt{2\pi}}e^{(-\frac{(x-\mu_x)^2)}{2\sigma_x^2})}, \frac{1}{\sigma_y\sqrt{2\pi}}e^{(-\frac{(y-\mu_y)^2)}{2\sigma_y^2})}\right) \tag{11}$$

.

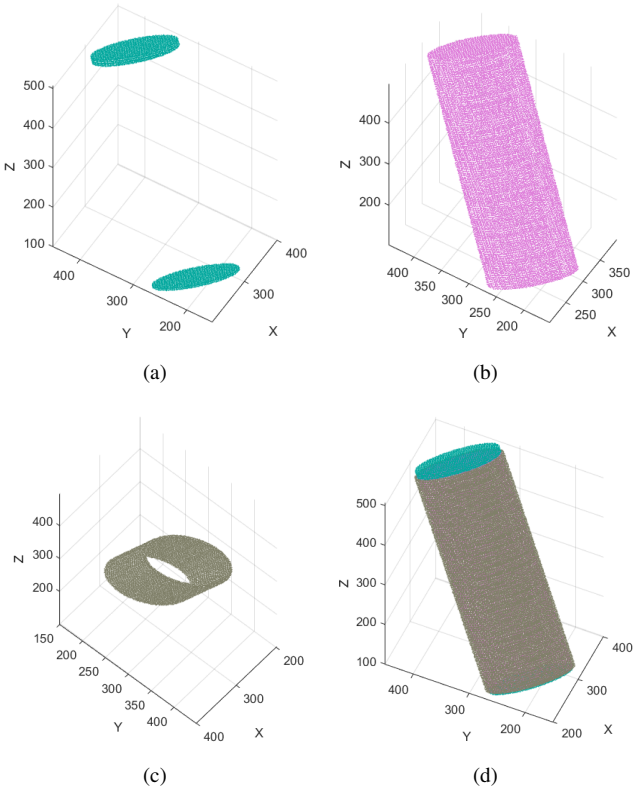

Fig. 4. Simulation of a myocyte with (a) the intercalated discs, (b) the cell, (c) the perimysium and (d) the whole myocyte.

IV. Results

We model three high-resolution geometric objects which shapes and size are inspired from human cardiac tissue data imaged in phase contrast (SR-PCT). The data provide from the left ventricle wall of two healthy adult hearts. Each sample of size $6\times6\times\times15mm^3$ and $6\times6\times\times20mm^3$ are reconstructed in 3D at an isotropic spatial resolution of $3.5\times3.5\times3.5\mu m^3$ [21], [25].

First, we simulate a myocyte that is the basic tissue unit of our model. We define its geometric shape as a simple cylinder with $L=100\mu m$ and an elliptic section of long axis $R_l=18\mu m$ and short axis $R_s=9\mu m$. We create the 3D voxel based model with a resolution of 0.25 μm/voxel with angles of 30^o against z axis and 60^o against the $x-y$ plane. We divide a myocyte into three parts: the cell, the perimysium and the intercalated discs as shown in Fig. 4. As the results show, we can process each part separately and combine them afterwards.

Second, we simulate the geometric model of a bundle. Based on this validated FFD pipeline, we perform a simulation of a bundle with several myocytes inside. We use a Voronoi diagram to generate compact myocytes in a bundle. For the FFD, we use a grid of 5×5 control points on each layer of the cylinder and calculate the local coordinates of the control points. The initial bundle has $R_b=30\mu m$ and $L_b=40\mu m$ with 7 myocytes generated inside. We generate an image with a resolution of 0.25 μm/pixel in each direction. The object shape

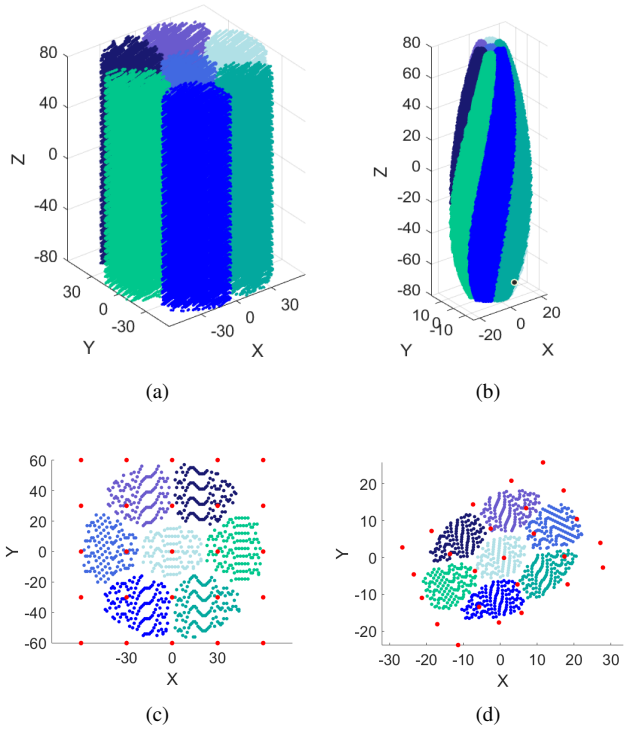

Fig. 5. Deformation from a bundle to a twisted truncated ellipsoid with noise. (a) the original bundle with 7 myocytes. (b) the result of the deformation which is a twisted truncated ellipsoid with noise. (c) the initial 40th layer of the cylinder with the 5×5 control points. (d) the deformed 40th layer with the moved, rotated and noisy control points.

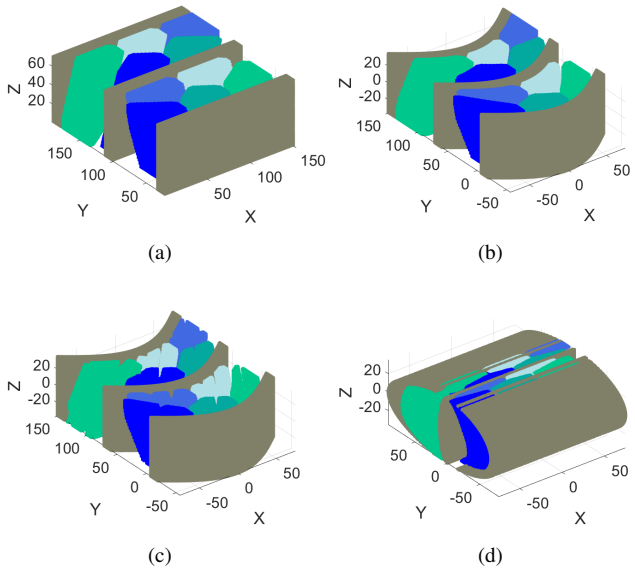

Fig. 6. Deformation of cleavage planes with bundles. (a) the original cleavage with bundles. (b) the curved cleavage planes with bundles. (c) the curved cleavage planes with bundles embedded myocytes (d) the merged cleavage planes with bundles.

is also a truncated ellipsoid with $R_x = 12.5\mu m$, $R_y = 8.75\mu m$ and $R_z = 22.5\mu m$ respectively. We also add a rotation (Eq. 10) and a Gaussian noise (Eq. 11) on each layer of the bundle, where $A_{rotation} = 1°/\mu m$, $\mu_x = 0$, $\mu_y = 0$, $\sigma_x = 3\mu m$ and $\sigma_y = 3\mu m$. From the results (Fig. 5), we see that the section at each layer is correctly transformed into an ellipse and because $R_z > L_b/2$, the ellipsoid is truncated at its two extremities in the z axis. We can clearly see that the deformed shape is the expected one and the free-form deformation keeps the gaps separating the myocytes.

After that, we use FFD to deform and merge cleavage planes as shown in Fig. 6. We start by simulating cleavage planes as some planes with thickness and putting some bundles between them. Through FFD, we can curve the cleavage planes with any curvatures as well as the bundles in them. Based on that, we use FFD to achieve merging and branching of cleavages planes. From these preliminary results, we confirm that the FFD technique is useful and effective to deform the cleavage planes and manipulate such complex biological shapes.

V. Discussion

In this paper, we build a geometric model coupled with FFD to deform it in several situations. However, during the FFD, the volume control is a challenge. In extreme deformation situations, the transformation is not isovolumic as for branching cleavage planes, which is a limitation. Because we use a voxel-based model and use the amount of voxels to denote the volume of an object, we cannot use the original Jacobian matrix to control the volume change during the deformation. Therefore, in our future work, we will use counting functions to control the volume change in order to finish the deformation under monitoring.

In our proposed multiscale model, we build five levels of elementary objects with the most basic unit being voxels. Thus, we will process the enormous amount of data and the trivial procedure.

Because it is a multiscale model, the shift between different scales is difficult to deal with. Since we currently have built models of single objects, the connection and arrangement of several objects will be the focus of our next step.

VI. Conclusion

We propose a multiscale synthetic model of the heart for virtual imaging. Our voxel-based model contains several elementary objects from macro- to micro-scale and necessary parameters to describe them. Currently we have built the structure of this model and geometric models for each elementary object. We introduce FFD into our model so that it can simulaterealistic data and the deformation during the cycle. In the future work, we will introduce statistics of the parameters, functional and dynamic information into our model in order to make it more realistic for virtual imaging. Moreover, the injection of experimental data as PLI [17] and SR-PCT [25], will increase the realistic rendering of the generated dataset.

Acknowledgment

Research conducted within the framework of the CNRS International Research Project METISLAB.

References

[1] D. Terzopoulos and D. Metaxas, "Dynamic 3d models with local and global deformations: Deformable superquadrics," *IEEE Transactions on Pattern Analysis & Machine Intelligence*, no. 7, pp. 703–714, 1991.

[2] J. Park, D. Metaxas, A. A. Young, and L. Axel, "Deformable models with parameter functions for cardiac motion analysis from tagged mri data," *IEEE Transactions on Medical Imaging*, vol. 15, no. 3, pp. 278–289, 1996.

[3] E. Bardinet, L. D. Cohen, and N. Ayache, "Tracking and motion analysis of the left ventricle with deformable superquadrics," 1996.

[4] P. A. Helm, H.-J. Tseng, L. Younes, E. R. McVeigh, and R. L. Winslow, "Ex vivo 3d diffusion tensor imaging and quantification of cardiac laminar structure," *Magnetic Resonance in Medicine: An Official Journal of the International Society for Magnetic Resonance in Medicine*, vol. 54, no. 4, pp. 850–859, 2005.

[5] R. L. Winslow, N. Trayanova, D. Geman, and M. I. Miller, "Computational medicine: translating models to clinical care," *Science translational medicine*, vol. 4, no. 158, pp. 158rv11–158rv11, 2012.

[6] H. Dejea, A. Bonnin, A. C. Cook, and P. Garcia-Canadilla, "Cardiac multi-scale investigation of the right and left ventricle ex-vivo : a review," *Cardiovascular Diagnosis and Therapy*, vol. 0, no. 0, 2020. [Online]. Available: http://cdt.amegroups.com/article/view/43224

[7] D. Tang, C. Yang, T. Geva, and J. Pedro, "Image-based patient-specific ventricle models with fluid–structure interaction for cardiac function assessment and surgical design optimization," *Progress in pediatric cardiology*, vol. 30, no. 1-2, pp. 51–62, 2010.

[8] K. Lekadir, B. Ghafaryasl, E. Muñoz-Moreno, C. Butakoff, C. Hoogendoorn, and A. F. Frangi, "Predictive modeling of cardiac fiber orientation using the knutsson mapping," in *International Conference on Medical Image Computing and Computer-Assisted Intervention*. Springer, 2011, pp. 50–57.

[9] S. Sugiura, T. Washio, A. Hatano, J. Okada, H. Watanabe, and T. Hisada, "Multi-scale simulations of cardiac electrophysiology and mechanics using the university of tokyo heart simulator," *Progress in biophysics and molecular biology*, vol. 110, no. 2-3, pp. 380–389, 2012.

[10] D. Ambrosi, A. Quarteroni, and G. Rozza, *Modeling of physiological flows*. Springer Science & Business Media, 2012, vol. 5.

[11] D. Sato and C. E. Clancy, "Cardiac electrophysiological dynamics from the cellular level to the organ level," *Biomedical engineering and computational biology*, vol. 5, pp. BECB–S10 960, 2013.

[12] N. A. Trayanova, "Whole-heart modeling: applications to cardiac electrophysiology and electromechanics," *Circulation research*, vol. 108, no. 1, pp. 113–128, 2011.

[13] V. Mihalef, R. I. Ionasec, P. Sharma, B. Georgescu, I. Voigt, M. Suehling, and D. Comaniciu, "Patient-specific modelling of whole heart anatomy, dynamics and haemodynamics from four-dimensional cardiac ct images," *Interface Focus*, vol. 1, no. 3, pp. 286–296, 2011.

[14] T. S. Eriksson, A. Prassl, G. Plank, and G. A. Holzapfel, "Influence of myocardial fiber/sheet orientations on left ventricular mechanical contraction," *Mathematics and Mechanics of Solids*, vol. 18, no. 6, pp. 592–606, 2013.

[15] R. Chabiniok, V. Y. Wang, M. Hadjicharalambous, L. Asner, J. Lee, M. Sermesant, E. Kuhl, A. A. Young, P. Moireau, M. P. Nash *et al.*, "Multiphysics and multiscale modelling, data–model fusion and integration of organ physiology in the clinic: ventricular cardiac mechanics," *Interface focus*, vol. 6, no. 2, p. 20150083, 2016.

[16] M. Smerup, E. Nielsen, P. Agger, J. Frandsen, P. Vestergaard-Poulsen, J. Andersen, J. Nyengaard, M. Pedersen, S. Ringgaard, V. Hjortdal *et al.*, "The three-dimensional arrangement of the myocytes aggregated together within the mammalian ventricular myocardium," *The Anatomical Record: Advances in Integrative Anatomy and Evolutionary Biology: Advances in Integrative Anatomy and Evolutionary Biology*, vol. 292, no. 1, pp. 1–11, 2009.

[17] P.-S. Jouk, B. L. Truong, G. Michalowicz, and Y. Usson, "Postnatal myocardium remodelling generates inhomogeneity in the architecture of the ventricular mass," *Surgical and Radiologic Anatomy*, vol. 40, no. 1, pp. 75–83, 2018.

[18] I. Mirea, "Analyse de la microstructure 3d du tissu cardiaque humain à l'aide de la micro-tomographie à rayons x par contraste de phase," Ph.D. dissertation, Lyon, 2017.

[19] I. Mirea, L. Wang, F. Varray, Y.-M. Zhu, E. D. Serrano, and I. E. Magnin, "Statistical analysis of transmural laminar microarchitecture of the human left ventricle," in *2016 IEEE 13th International Conference on Signal Processing (ICSP)*. IEEE, 2016, pp. 53–56.

[20] F. Varray, I. Mirea, M. Langer, F. Peyrin, L. Fanton, and I. E. Magnin, "Extraction of the 3d local orientation of myocytes in human cardiac tissue using x-ray phase-contrast micro-tomography and multi-scale analysis," *Medical image analysis*, vol. 38, pp. 117–132, 2017.

[21] S. Wang, I. Mirea, F. Varray, W.-Y. Liu, and I. E. Magnin, "Investigating the 3d local myocytes arrangement in the human lv mid-wall with the transverse angle," in *International Conference on Functional Imaging and Modeling of the Heart*. Springer, 2019, pp. 208–216.

[22] M. Caon, "Voxel-based computational models of real human anatomy: a review," *Radiation and environmental biophysics*, vol. 42, no. 4, pp. 229–235, 2004.

[23] T. W. Sederberg and S. R. Parry, "Free-form deformation of solid geometric models," in *Proceedings of the 13th annual conference on Computer graphics and interactive techniques*, 1986, pp. 151–160.

[24] I. LeGrice, P. Hunter, A. Young, and B. Smaill, "The architecture of the heart: a data–based model," *Philosophical Transactions of the Royal Society of London. Series A: Mathematical, Physical and Engineering Sciences*, vol. 359, no. 1783, pp. 1217–1232, 2001.

[25] I. Mirea, F. Varray, Y. M. Zhu, L. Fanton, M. Langer, P.-S. Jouk, G. Michalowicz, Y. Usson, and I. E. Magnin, "Very high-resolution imaging of post-mortem human cardiac tissue using x-ray phase contrast tomography," in *International Conference on Functional Imaging and Modeling of the Heart*. Springer, 2015, pp. 172–179.